







# Treatment with shRNA to knockdown the 5-HT<sub>2A</sub> receptor improves memory *in vivo* and decreases excitability in primary cortical neurons

Troy T. Rohn<sup>1</sup> , Dean Radin<sup>1</sup> , Tracy Brandmeyer<sup>1</sup> ,  
 Peter G. Seidler<sup>1</sup> , Barry J. Linder<sup>1</sup>, Tom Lytle<sup>1</sup>, David Pyrce<sup>1</sup>,  
 John L. Mee<sup>1</sup> , and Fabio Macchiardi<sup>1,2</sup> 

<sup>1</sup>Cognigenics, Eagle, Idaho, 83616, USA

<sup>2</sup>Department of Psychiatry and Human Behavior, University of California, Irvine, California 92697, USA

**Corresponding Author:** Troy T. Rohn, 1372 S. Eagle Road, Suite 197  
 Eagle, Idaho 83616 USA. E-mail: [troy.rohn@cognigenics.io](mailto:troy.rohn@cognigenics.io)

*Genomic Psychiatry*; <https://doi.org/10.61373/gp024r.0043>

**Short hairpin RNAs (shRNA), targeting knockdown of specific genes, hold enormous promise for precision-based therapeutics to treat numerous neurodegenerative disorders. We designed an AAV9-shRNA targeting the downregulation of the 5-HT<sub>2A</sub> receptor, and recently demonstrated that intranasal delivery of this shRNA (referred to as COG-201), decreased anxiety and enhanced memory in mice and rats. In the current study, we provide additional *in vivo* data supporting a role of COG-201 in enhancing memory and functional *in vitro* data, whereby knockdown of the 5-HT<sub>2A</sub> receptor in primary mouse cortical neurons led to a significant decrease in mRNA expression ( $p = 0.0007$ ), protein expression  $p$ -value = 0.0002, and in spontaneous electrical activity as measured by multielectrode array. In this regard, we observed a significant decrease in the number of spikes ( $p$ -value = 0.002), the mean firing rate ( $p$ -value = 0.002), the number of bursts ( $p$ -value = 0.015), and a decrease in the synchrony index ( $p$ -value = 0.005). The decrease in mRNA and protein expression, along with reduced spontaneous electrical activity in primary mouse cortical neurons, corroborate our *in vivo* findings and underscore the efficacy of COG-201 in decreasing *HTR2A* gene expression. This convergence of *in vitro* and *in vivo* evidence solidifies the potential of COG-201 as a targeted therapeutic strategy. The ability of COG-201 to decrease anxiety and enhance memory in animal models suggests that similar benefits might be achievable in humans. This could lead to the development of new treatments for conditions like generalized anxiety disorder, post-traumatic stress disorder (PTSD), and cognitive impairments associated with aging or neurodegenerative diseases.**

**Keywords:** RNA interference, 5-HT<sub>2A</sub> receptor, memory enhancement, neuronal excitability, anxiety, cognitive impairment.

## Introduction

Neurological disorders such as mild cognitive impairment (MCI) and chronic anxiety are a major public mental health challenge, affecting millions of people worldwide. MCI is often a transitional stage between healthy aging and dementia. Depending on the inclusion criteria, the prevalence of MCI has been estimated to be between 5.0% and 36.7% (1). According to a systematic review and meta-analysis, the overall pooled prevalence of anxiety in patients with MCI is approximately 21%. This prevalence rate varies based on the source of the sample and the method of diagnosis. For example, the prevalence of anxiety in community-based samples of patients with MCI is about 14.3%, while it is approximately 31.2% in clinic-based samples (2). Based on these statistics, we estimate

that roughly 1.5–2 million Americans suffer from MCI with an underlying anxiety disorder. Currently, there is no single medication to treat both cognitive impairments and anxiety in this patient population.

Precision-based therapeutics such as RNA interference offer a promising new approach to treating neurological and neurodegenerative disorders. Short hairpin RNA (shRNA) represents one class of RNA interference molecules that has a mechanism based on the sequence-specific degradation of host mRNA through cytoplasmic delivery and degradation of double-stranded RNA through the RNA-induced silencing complex (RISC) pathway (3, 4). We designed plasmids containing the RNA instructions to construct a specific shRNA to silence the *HTR2A* gene (U.S. Patent Application No. 63/567,853). The *HTR2A* gene encodes for the 5-HT<sub>2A</sub> receptor, one of the 15 known serotonin receptor subtypes expressed in the brain, and is implicated in both anxiety disorders (5, 6) and memory (7–9). This plasmid contains a neuronal specific promoter, MeCP2 and is packaged within AAV9 viral particles. Intranasal treatment of this AAV9-shRNA (herein termed COG-201) in mice or rats significantly decreased anxiety and improved memory (10). In this study, we present further evidence supporting the memory-enhancing effects COG-201. We also provide functional data from experiments on primary cortical neurons taken from mice. Our results show that treatment with COG-201 leads to reduced spontaneous electrical activity in these neurons. This effect occurs specifically after reducing the expression of the 5-HT<sub>2A</sub> receptor. These findings bolster the potential of intranasal shRNA delivery as a non-invasive therapeutic method and establish a foundation for continued investigation into its role in treating anxiety and cognitive deficits linked to a spectrum of neurodegenerative diseases.

## Methods

### shRNA Design and AAV9 Vector Design

Construction of the mouse shRNA to target knockdown of the 5-HT<sub>2A</sub> receptor was as previously described (11). The mouse *HTR2A* gene consists of three exons that give rise to two major isoforms and is found on chromosome 13. The predicted binding region of the primary RNA transcript for this sequence is the beginning of exon 2, which would lead to the potential knockdown of all possible isoforms. The following sequence was used for assembly of the shRNA based on *in vitro* testing indicating a 77% knockdown:

```
GCTGAGCACATCCAGGTAATCCAGGTTTGGCCACGACTGACCTGGATT  
CTGGATGTGCT CAG
```

No knockdown was observed with the empty vector control or a scrambled shRNA control (Figure 2B). For validation and screening, knockdown was verified using HEK293 cells cotransfected with the cDNA plasmid containing the *HTR2A* gene target. For *in vitro* treatment of primary mouse cortical neurons, shRNA delivery subcloning of the shRNA was carried out in a modified pAAV *cis*-plasmid under the neuronal-specific promoter, MeCP2. The inclusion of the MeCP2 promoter is a crucial element design, as it ensures expression of the shRNA plasmid only in neuronal populations. A reporter gene enhanced green fluorescent protein was subcloned upstream of the shRNA sequence. AAV9 viral large-scale transfection of plasmids was carried out in HEK293 cells and purified through a series of CsCl centrifugations. Titer load (in genome copy number per mL, or GC/mL) was determined through quantitative real-time PCR, with typical yields giving 1–2 × 10<sup>13</sup> GC/mL. All AAV9 vectors were stored in phosphate buffered saline (PBS) with 5% glycerol at –80°C until used. Design, manufacturing, and purification of AAV9 vectors used in this study were performed by Vector Biolabs (Malvern, PA).

### Novel Object Recognition Test

The object recognition task is used to assess short-term memory, intermediate-term memory, and long-term memory in rats and was performed as previously described (11). The task is based on the natural tendency of rats to preferentially explore a novel versus a familiar object, which requires memory of the familiar object. The time delay design allows for the screening of compounds with potential cognitive enhancing





properties to overcome the natural forgetting process. Wistar male rats (12 animals per group) were randomly assigned to two groups consisting of vehicle (PBS) or COG-201 treated. Following administration of the vehicle or COG-201, rats were assessed in this task 3 weeks posttreatment and the discrimination index was calculated. To calculate the discrimination index, the following equation was used: (time exploring novel object-time exploring familiar object)/(time exploring novel object + time exploring familiar object), multiplied by 100 to convert to a percentage. The arena and objects were cleaned with 70% alcohol between each rat test session. These behavioral studies were performed by Neurofit SAS. All animal care and experimental procedures were performed in accordance with institutional guidelines and were conducted in compliance with French Animal Health Regulation. For all behavioral studies, animals were keyed, and data were blinded until the end of experiments.

#### Primary Mouse Cortical Neuron Cultures and Treatment with COG-201

Primary cortical neurons from fresh mouse brain embryos were isolated and plated onto coated 24-well plates at a density of  $5 \times 10^5$  cells/well. Cortical neurons were maintained in Neurobasal-A Medium, supplemented with B27, Glutamax, and antibiotics (100 U/MI penicillin and 100  $\mu$ g/mL streptomycin). Cultured neurons were incubated at 37°C and 5% CO<sub>2</sub> and half the media were exchanged with fresh, complete media every 3 days. On day 6 following plating (DIV 6), cortical neurons were treated exogenously with a stock concentration of COG-201 at  $1 \times 10^{13}$  (GC/mL) to a final multiplicity of infection (MOI) of  $2 \times 10^5$ . The MOI refers to the number of viral particles per neuron. Alternatively, cortical neurons were treated at the same MOI using AAV9-MeCP2-GFP-scrambled-shRNA representing the *HTR2A* target sequence but randomly scrambled. Cultured neuronal media was replaced with half, fresh, complete media every 3 days for 10 days (DIV 16) at which point cells were fixed for immunocytochemistry or analyzed for spontaneous electrical activity via MEA. Preparation and maintenance of primary mouse cortical neuron cultures was carried out by Creative Biolabs (Shirley, NY).

#### Ethical Animal Treatment Statement

Creative Biolabs complies with all provisions of the Animal Welfare Act and other regulations related to animals. Every individual involved in the care and use of laboratory animals fully understands the responsibilities, such as: avoids or minimizes discomfort, distress, and pain in experimental animals consistent with sound scientific practices; uses minimum number of animals necessary to obtain valid results. All experimental protocols were approved by the relevant Institutional Animal Care and Use Committee.

#### Immunohistochemical Fluorescence Microscopy

Immunofluorescence histochemistry was as previously described (10, 11). Briefly, following dehydration, 4  $\mu$ m paraffin-embedded, sagittal sections were cut just lateral to the midline and used for immunofluorescence labeling. Briefly, all tissue sections were labeled with anti-GFP antibody (rabbit mAb #2956) 1:1,000 (Cell Signaling Technology, Inc., Danvers, MA, USA) or anti-5HT-2A receptor antibody (rabbit polyclonal, #24288) at 1:500 dilution (Immunostar, Hudson, WI). Secondary antibodies were conjugated to FITC or Cy3. DAPI was used as a nuclear stain. Whole slide scanning was performed using a Panoramic Midi II scanner using a 40X objective lens with optical magnification of 98X, 0.1  $\mu$ m/pixel. All sectioning, immunolabeling, and capturing of images was contracted out to iHisto (Salem, MA).

#### Immunocytochemistry Protocol

Cells were cultured under appropriate conditions before the immunocytochemistry procedure was initiated. For fixation, cells were treated with 4% paraformaldehyde prepared in 1x PBS. The fixation solution was preheated to 37°C prior to use. Cells were incubated with this solution for 10 minutes at room temperature to preserve cellular architecture and antigenicity. Following fixation, cells were washed thrice with 1x PBS, with each wash lasting for 3 minutes, to remove excess fixative. To permeabilize the cell membranes, 0.1% Triton X-100 (diluted in PBS) was added to the wells, and the cells were incubated for 15 minutes at room temperature. This step facilitates the entry of antibodies into the cells. Subsequently, cells were again washed three times with 1x PBS for 3 minutes each to remove the permeabilization agent.

The cells were then blocked with 500  $\mu$ L of ready-to-use goat serum for 1 hour at room temperature to prevent non-specific binding of the primary antibodies. After blocking, the primary antibodies were diluted in the goat serum; GFP monoclonal antibody from mouse was diluted at 1:500, and 5HT2A antibody from rabbit at 1:100. The primary antibody solution was added to the wells, and the cells were incubated overnight at 4°C. The next day, the cells were washed three times with 1x PBS for 3 minutes each to remove unbound primary antibodies. The secondary antibodies were then prepared: AF488 Goat anti-Mouse IgG (H+L) and AF555 Goat anti-Rabbit IgG (H+L), both diluted at 1:400 in goat serum. The secondary antibody solution was added to the wells, and cells were incubated for 2 hours at room temperature in the dark to protect the fluorophores from photobleaching. After incubation with the secondary antibodies, cells were washed with 1x PBS to remove any unbound antibodies. Subsequently, nuclei were stained with a Hoechst solution, which was added directly to the wells. The cells were incubated in the dark for 5–10 minutes, followed by a final wash with PBS. Finally, the stained cells were imaged using appropriate fluorescence microscopy to detect the signals from the fluorophore-conjugated antibodies. Upon completion of imaging, the slides were sealed to prevent drying and to preserve the fluorescence for future analysis. Immunocytochemistry was performed by Creative Biolabs (Shirley, NY, USA).

#### Western Blot Analysis Protocol

Following treatment, proteins were extracted from cortical neurons the protein concentration was determined using a standard protein assay. Equal amounts of protein from each sample were then diluted with PBS to normalize the volume across all samples. The samples were mixed with loading buffer at a 1:4 volume ratio and denatured by heating at 100°C for 10 minutes. For electrophoresis, samples were loaded into a precast polyacrylamide gel alongside a molecular weight marker. The proteins were then transferred onto a polyvinylidene difluoride (PVDF) membrane using a semi-dry transfer system. Posttransfer, the PVDF membrane was blocked in 5% non-fat milk prepared in Tris-buffered saline with Tween 20 (TBST) to prevent non-specific protein binding. Subsequently, the membrane was incubated with a primary antibody against the 5-HT2A receptor, diluted to a concentration of 0.3  $\mu$ g/mL, and placed overnight at 4°C on a shaker. The membrane was washed three times with TBST for 10 minutes and then incubated with a goat anti-rabbit secondary antibody solution for 1 hour at room temperature on a shaker. For the detection of the antibody-protein complex, a chemiluminescent substrate was prepared and added to the membrane, which was then incubated for 5 minutes. The intensity of the bands was analyzed by densitometry to determine the relative amounts of the target protein present in the samples. Western blot analysis was performed by Creative Biolabs (Shirley, NY, USA).

#### Quantitative Real-time qPCR

Real-time qPCR was performed as previously described (11). Briefly, total RNA was extracted from primary cortical mouse neurons using a standard extraction protocol with TRIzol, dissolved in diethyl pyrocarbonate (DEPC)-treated deionized water and quantified. Following reverse transcription, qPCR was carried out using the following primers: Primer-F: 5'-AGAGGAGCCACACAGGTCTC-3' and Primer-R: 5'-ACGACAGTTGTCAATAAAGCAG-3'. The relative expression was determined by calculating the  $2^{-\Delta\text{ct}}$  value. The  $2^{(-\text{ddCt})}$  value was then calculated and normalized to GAPDH for each treatment (AAV9-scrambled vs. COG-201). The RNA extraction and qPCR were performed by Creative Biogene (Shirley, NY, USA).

#### Multielectrode Array Analysis

MEA analysis was performed as previously described (11). Briefly, the microscope used was an Evos XL Core. Twenty-four-well MEA plates were coated with 500  $\mu$ L 0.07% polyetherimide (PEI) and incubated for 1 hour. Plates were then washed four times in sterile deionized water and dried overnight in a biosafety cabinet. Primary cortical neurons from fresh mouse brain embryos were isolated and plated onto coated 24-well plates at a density of  $5 \times 10^5$  cells/well. Cortical neurons were maintained in Neurobasal-A Medium, supplemented with B27, Glutamax, and antibiotics (100 U/MI penicillin and 100  $\mu$ g/mL streptomycin). Cultured neurons were incubated at 37°C and 5% CO<sub>2</sub> and half the media were exchanged



with fresh, complete media every 3 days. Treatment (MOI of  $2 \times 10^5$ ) occurred on day 6 for 24 hours at 37°C at which time the media was replaced with fresh, complete media. MEA analysis was then performed on day 16, 10 days after infection. MEA analysis was performed by Creative Biolabs (Shirley, NY).

#### Statistical Analysis

For PCR, and Western blot quantification, *t* tests for two independent means were calculated using excel software using a significance level set at 0.05 and one-tailed hypotheses. Microelectrode array data were analyzed via repeated measures ANOVAs using Statistica (Version 13.5, Tibco Software). All data used in these tests were checked and found to conform to parametric assumptions.

#### Acknowledgment of Generative Artificial Intelligence and Artificial Intelligence–assisted Technologies Used in Writing

In the course of this work's preparation, the author(s) employed ChatGPT 4 with the intent to improve readability and language. Upon utilizing this tool/service, the authors undertook comprehensive review and modification as necessary and assume full accountability for the content of the publication.

#### Results and Discussion

In a recent study, we have demonstrated a decrease in anxiety and improvement in memory following intranasal delivery of COG-201 in rats or mice (10). In that study, a novel recognition object test in normal, 2-month-old rats were carried out following treatment with COG-201. We reported a significant increase in both the contact-recognition index (92%) and time-recognition index (73%). In the current study, we now report a significant increase in the discrimination index in the novel recognition object test 3 weeks posttreatment with COG-201 (Figure 1A), and knockdown of the 5-HT<sub>2A</sub> receptor (Figure 1C) following intranasal delivery. The discrimination index is a measure used in the novel object recognition test to quantify the difference in exploration time between a novel and a familiar object. A positive discrimination index suggests that the animal spent more time exploring the novel object, which implies recognition of the familiar object and, thus, intact memory. Figure 1A indicates the vehicle-treated group exhibited a  $-28.9\%$  discrimination index, which suggests that, on average, the rats spent more time with the familiar object than with the novel object during the retention test. One interpretation of these results is that the control group either did not remember the familiar object or there was an alternative factor at play (e.g., anxiety, stress). In contrast to the control group, the rats treated with COG-201 displayed a discrimination index increase of 22.5%. Thus, on average, treated rats dedicated more time to interacting with a new object rather than a familiar one, indicative of enhanced memory retention. The positive effects of COG-201 on memory retention are further highlighted when considering the significant negative discrimination index observed in the group treated with the vehicle alone. The contrast between the groups could suggest that COG-201 not only improves memory retention directly but may also improve it indirectly by reducing anxiety, or through a synergistic effect of both mechanisms.

These results, taken together with our previous findings support a memory enhancement action of COG-201. However, the missing component is functional data connecting the knockdown of the 5-HT<sub>2A</sub> receptor to the behavioral actions of COG-201. An additional aim of the current study was to provide functional data to support these behavioral findings. The serotonin 5-HT<sub>2A</sub> receptor is the major excitatory receptor subtype in the cortex. For example, this receptor has been linked with stress-induced dystonia, emphasizing its role in mediating neuronal excitability (12). In addition, the 5-HT<sub>2A</sub> receptor has been associated with excitatory effects in the neocortex and has been linked to working memory function by influencing both excitatory and inhibitory elements within local circuitry (13). Moreover, the 5-HT<sub>2A</sub> receptor has been found to directly stimulate key excitatory glomerular neurons in the olfactory bulb, further supporting its role in excitatory synaptic transmission (14). Overall, the 5-HT<sub>2A</sub> receptor plays a crucial role in memory, anxiety, and pain modulation, exerting excitatory effects in these processes. Therefore, we examined whether exposure of COG-201 to primary culture

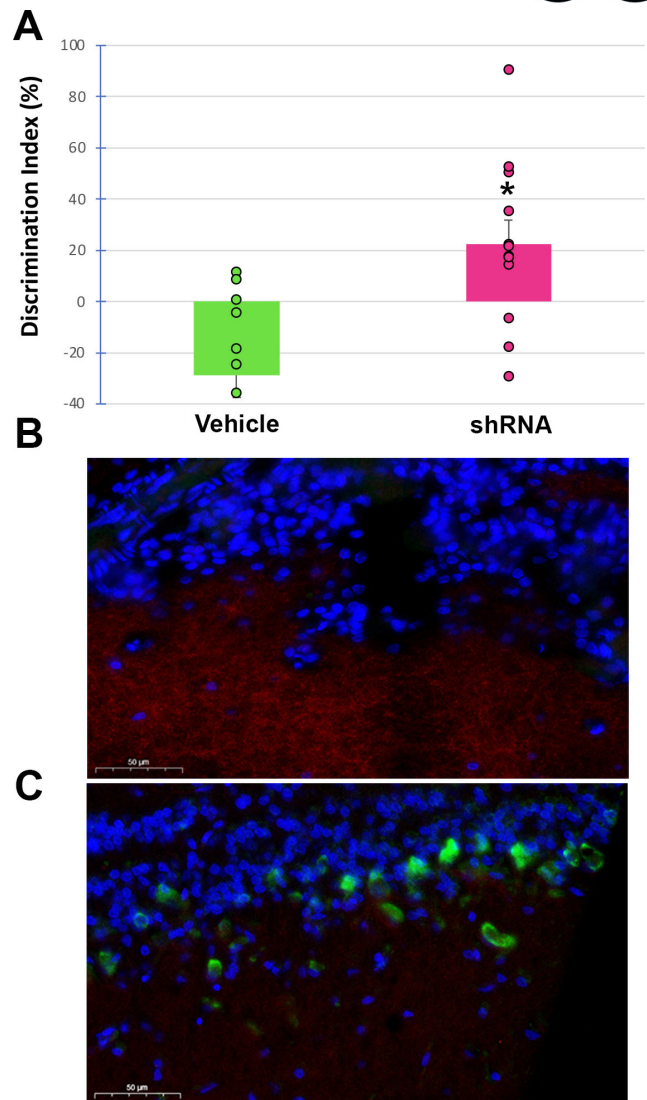


**Figure 1.** Intranasal adeno-associated virus delivery of AAV9-MeCP2-GFP-mouse HTR2A-shRNA improves memory in rats. The target sequence used to synthesize the shRNA is 100% conserved between mice and rats. To test whether COG-201 knockdown of the rat 5-HT<sub>2A</sub> receptor improves memory, Wistar rats (12 animals per group) were randomly assigned to two different groups consisting of vehicle-controls or COG-201. Following treatment on day 1, animals were assessed behaviorally 3 weeks later, and the discrimination index was calculated (see *Methods* for details). (A) At 3 weeks, there was a significant difference in the discrimination index between the two groups (*p*-value = .00025), with the vehicle controls at  $-28.8\%$  (green bar) versus COG-201-treated  $+22.5\%$  (pink bar). The green bar (labeled "Vehicle") shows the performance the control group. This group's discrimination index is around  $-20\%$ , indicating a failure of preference for the novel object over the familiar one. This indicates poor performance in recognizing the new object. On the other hand, the pink bar (labeled "shRNA") represents the group of mice that received treatment with shRNA. Their discrimination index is around 30%, meaning they spent significantly more time exploring the novel object compared to the familiar one. This indicates better performance in recognizing the new object. (B and C) Representative, merged immunofluorescence image of vehicle-control animals depicting the presence of 5-HT<sub>2A</sub> receptor protein labeling (red fluorescence) within the olfactory bulb. The blue staining reflects nuclear staining with DAPI. As expected, there was no expression of GFP in vehicle controls (B) while strong GFP labeling was observed in cell bodies of neurons of shRNA-treated rats (C). Panel C also depicts a general lack of 5-HT<sub>2A</sub> fluorescence, supporting a knockdown of the receptor following COG-201 treatment. Images are representative of 3 separate rats for each group.

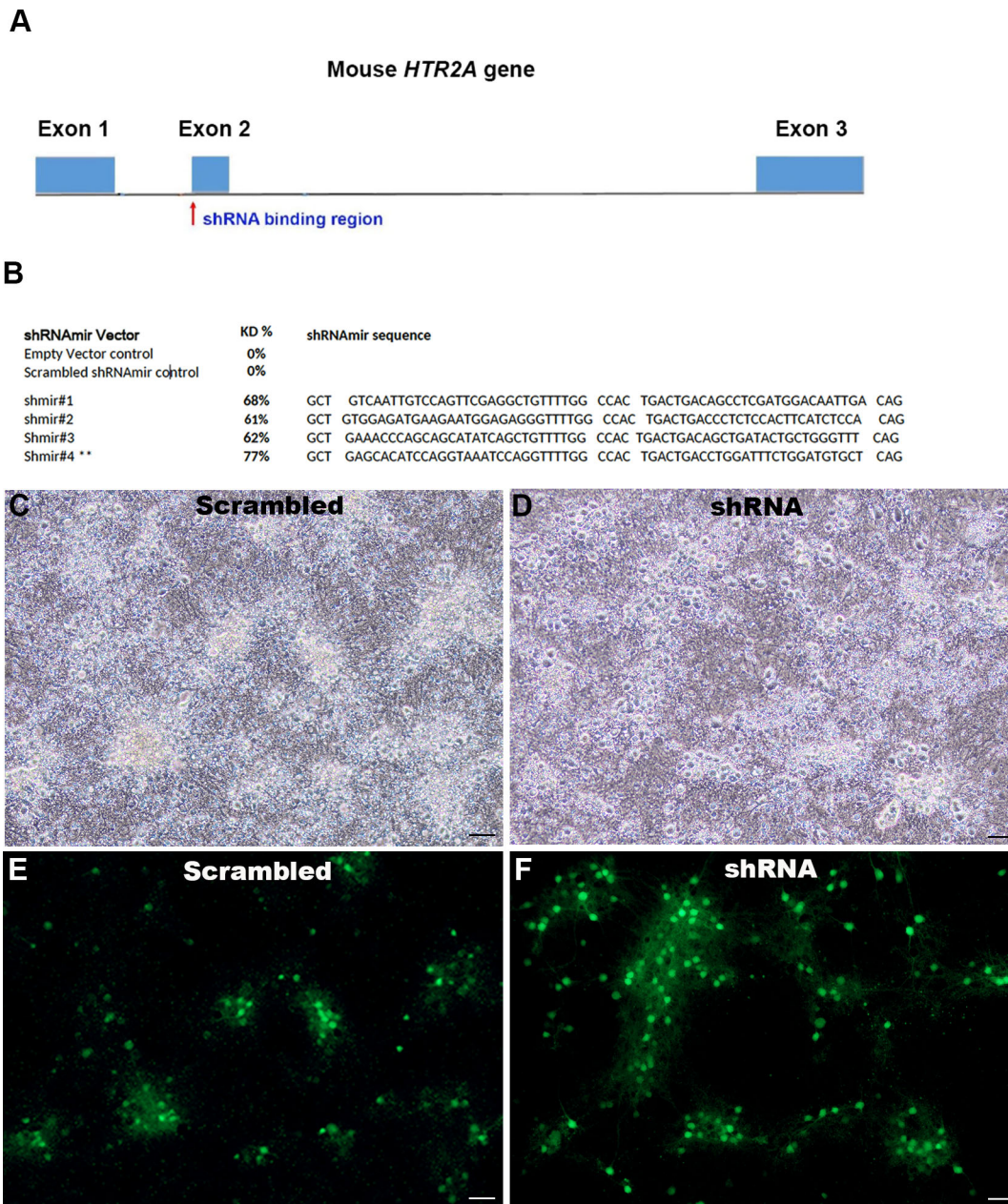


**Figure 2.** Targeting strategy to knock down the mouse *HTR2A* gene using shRNA and transduction efficiency in primary mouse cortical neurons. **(A)** Schematic displaying the *HTR2A* mouse gene encodes a single protein-coding transcript, *Htr2a-201*, located on chromosome 14 (11). The target sequence was constructed to recognize the beginning of exon 2 (red arrow, A). Knockdown of exon 2 prevent the production of all known full-length isoforms of the 5-HT<sub>2A</sub> receptors in mice. **(B)** To verify knockdown, *in vitro* experiments were undertaken using four different shRNAs, with shmir#4 giving the largest percent knockdown of *HTR2A* mRNA (77%) compared to 0% knockdown for either the empty vector control or a scrambled shRNA control. **(C–F)** Transduction efficiency of AAV9-mHTR2A-shRNA in mouse primary cortical neurons. **(C and D)** depict representative microscopic images in mouse neurons following a 10-day treatment with scrambled AAV9 shRNA-AAV9 viral particles **(C and D)** or mHTR2A shRNA-AAV9 viral particles at a MOI of  $2 \times 10^5$  **(D and F)**. Panels C and D represent bright-field images while Panels E and F are fluorescence images representing green fluorescence protein expression. For both constructs, strong GFP expression was observed.

neurons would lead to a decrease in electrical activity as measured by MEA. In this case, we measured the spontaneous activity of networks following treatment by recording field potentials. The advantage of MEA is that it can generate high-throughput readout of neuronal populations with the placement of multiple electrodes recording all at once rather than individually.

As an initial approach, we determined the relative transduction efficiency in primary cultured mouse neurons following *in vitro* treatment with either COG-201, or a scrambled AAV9-shRNA version. **Figure 2A** outlines the *HTR2A* gene targeting strategy, where shRNA is designed to bind

at the start of exon 2, effectively halting the synthesis of all known full-length 5-HT<sub>2A</sub> receptor isoforms. **Figure 2B** demonstrates the efficacy of our targeted silencing approach, where shmir#4 induced a 77% decrease in *HTR2A* mRNA levels. This reduction is in stark contrast to the negligible impact observed with the scrambled shRNA control. The comparison was made in HEK293 cells that were cotransfected with a cDNA plasmid specifically engineered to contain the *HTR2A* gene sequence targeted by the shRNAs. As expected, following treatment of mouse primary cortical neurons, high transduction efficiency of AAV9-mediated shRNA delivery for both the AAV9-scrambled shRNA (**Figure 2E**) and COG-201

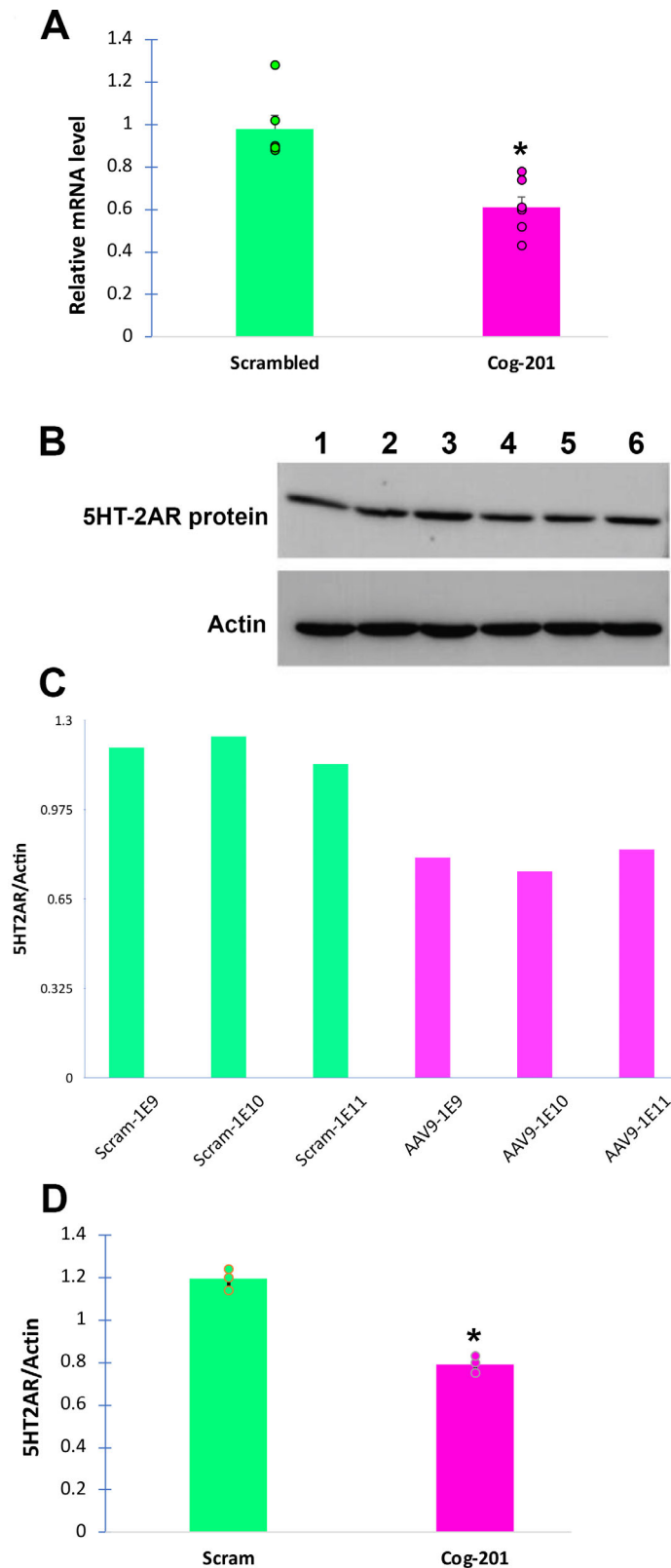


**Figure 3.** Treatment of mouse primary cortical neurons with shRNA leads to knockdown of the 5-HT<sub>2A</sub> receptor. Primary cortical neurons were treated on day 6 of plating with scrambled AAV9 shRNA-AAV9 viral particles (A) or COG-201 (B) at MOI of  $3 \times 10^5$  for 10 days (day 16, 10 dpi) at which time, mRNA was isolated for real-time qPCR experiments. Results display the relative change in expression using GAPDH (Continued on the next column)

(Continued) as an internal control. Real-time qPCR results represent a total of three separate treatments for each condition in which cells were pooled and frozen at  $-80^{\circ}\text{C}$ . PCR experiments were performed in triplicate. The results indicated a significant 38% decrease in HTR2A mRNA expression as compared to vehicle controls,  $p = .0007$ . (B–D) Cortical neurons were treated at various concentrations and cell homogenates were prepared for Western blot analysis. Transferred membranes were incubated with  $0.3 \mu\text{g}/\text{mL}$  of anti-5HT<sub>2A</sub> receptor antibody overnight at  $4^{\circ}\text{C}$  followed by goat anti-rabbit secondary antibody for 1 hour at room temperature. Panel B displays the results indicating 5-HT<sub>2AR</sub> protein band in scrambled-treated neurons (lanes 1–3) or in AAV9-shRNA-treated neurons (lanes 4–6). Densitometry analysis indicated a decrease in band intensity for COG-201 treated neurons (C). In panel D, data from lanes 1–3 and 4–6 were combined and the resulted data indicated an overall 34% decrease in 5-HT<sub>2A</sub> receptor protein in treated neurons versus scrambled controls ( $p$ -value = .0002).

(Figure 2F) was observed by fluorescence microscopy, as indicated by robust GFP expression.

We next determined the extent of 5-HT<sub>2A</sub> receptor knockdown by real-time qPCR or Western blot analysis (Figure 3). In this investigation, primary cortical neurons underwent treatment with shRNA to assess the knockdown of the 5-HT<sub>2A</sub> receptor expression, as illustrated in Figure 3. Neurons treated with COG-201 exhibited a significant 38% reduction in HTR2A mRNA expression as compared to the scrambled AAV9 shRNA-AAV9 controls, a finding confirmed by real-time qPCR with GAPDH as a reference ( $p = 0.0007$ ). This knockdown of HTR2A mRNA was further substantiated at the protein level through Western blot analysis. After incubation with anti-5HT<sub>2A</sub> receptor antibody, the resulting combined densitometry results revealed a corresponding 34% decrease in 5-HT<sub>2A</sub> receptor protein levels in neurons treated with COG-201, as compared to scrambled controls (Figure 3C and D), ( $p$ -value = 0.0002), thus confirming the knockdown at both transcriptional and translational levels.

Further confirmation of 5-HT<sub>2A</sub> receptor knockdown by COG-201 was obtained by immunocytochemistry. Neurons treated with scrambled AAV9-shRNA viral particles showed strong expression of the 5-HT<sub>2A</sub> receptor protein, as evidenced by the robust red fluorescence (Figure 4A and D). In contrast, neurons treated with COG-201 exhibit a marked decrease in 5-HT<sub>2A</sub> receptor expression (Figure 4E and H), indicating successful receptor knockdown. Collectively, the results presented in Figures 3 and 4 confirm the successful targeting and subsequent knockdown of the 5-HT<sub>2A</sub> receptor by COG-201, establishing the rationale for the next phase of the study, where we aimed to elucidate the implications of 5-HT<sub>2A</sub> receptor knockdown on neuronal excitability employing MEA analysis.

To accomplish this, primary cortical neurons were treated on day 6 with COG-201 or the scrambled AAV9-shRNA version and spontaneous electrical activity (MEA measurements) were recorded 10 days later. Several parameters were measured including (a) the number of spikes (Figure 5A), which is defined as the total count of action potentials (spikes) recorded by the MEA over a 5-minute period, where each spike is a brief electrical impulse that represents a single neuronal firing event; (b) the mean firing rate (Figure 5B) defined as the average rate at which a neuron fires action potentials (spikes) measured in hertz (Hz); (c) the number of bursts (Figure 5C), defined as a cluster of action potentials (spikes) that occurs in quick succession, followed by a period of silence; (d) the synchrony index (Figure 5D), defined as how in sync the firing of different neurons or groups of neurons is with values closer to 1 indicating strong synchrony; (e) number of network bursts (Figure 5E) representing coordinated activity across the neural network, thought to be crucial for various neural processes, including learning and memory and are indicative of the network's ability to engage in coordinated processing and communication; and finally, (f) the number of active electrodes (Figure 5F). A higher number of active electrodes typically suggests a more widespread or synchronized activity across the network, indicating robust interneuronal communication and network integration. To summarize the results in Figure 5, we observed a significant decrease in the

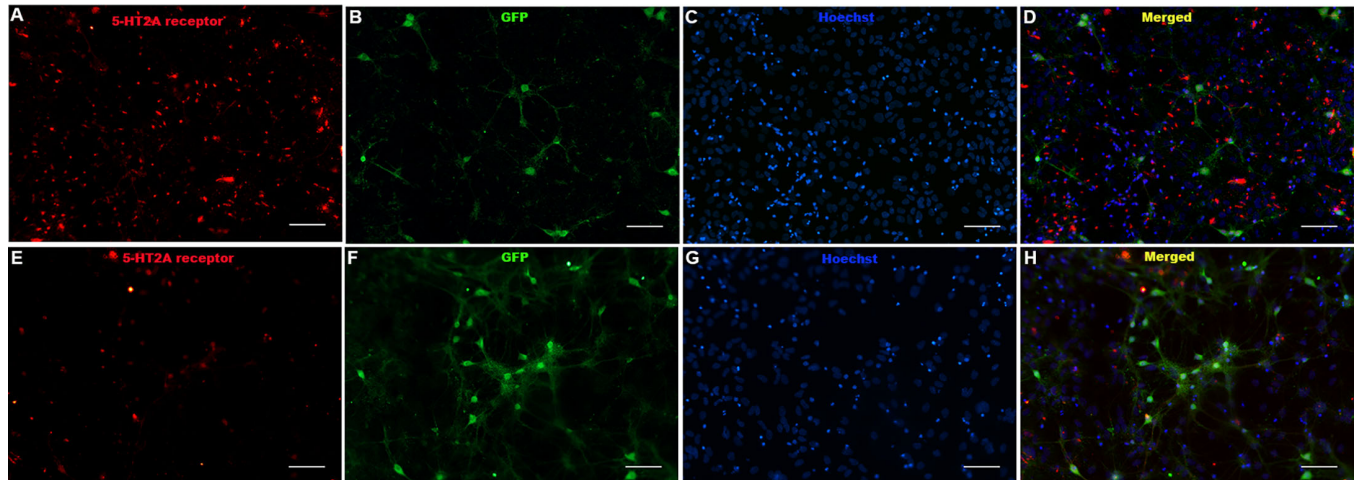


**Figure 4.** Treatment of mouse primary cortical neurons with COG-201 leads to knockdown of the 5-HT<sub>2A</sub> receptor. Representative immunofluorescence images in mouse neurons following a 10-day treatment with either scrambled AAV9 shRNA-AAV9 viral particles (**A–D**) or COG-201 at MOI of  $3 \times 10^5$  (**E–H**). Green fluorescence represents green fluorescence protein expression detected using a GFP monoclonal antibody (mouse, 1:500) (**B** and **F**), while red fluorescence is indicative of 5-HT<sub>2A</sub> receptor protein following immunocytochemistry using an anti-rabbit 5-HT<sub>2A</sub> receptor antibody (Immunostar, 1:100). Panel **A** and **D** display robust expression of the 5-HT<sub>2A</sub> receptor protein in neuronal cells following treatment with the scrambled control. In contrast, a significant reduction in 5-HT<sub>2A</sub> fluorescence intensity was evident following treatment with COG-201 (**E** and **H**). Panels **C** and **G** represent Hoechst nuclear labeling while panels **D** and **H** represent merged images. All scale bars represent 50  $\mu$ m.

number spikes, mean firing rate, number of bursts, and synchrony index but an increase in the number of network bursts following treatment with COG-201 in non-stimulated neurons. These data could be interpreted to suggest that a reduction in overall excitability supported the actions of COG-201 on knockdown of the excitatory 5-HT<sub>2A</sub> receptor. In addition, the significant decrease in the number of bursts of isolated neurons and in the synchrony index suggests that neurons with a reduced expression of 5-HT<sub>2A</sub> present with a lower frequency of spontaneous electrical activity (from 1.2 to  $\sim$ 6 Hz). On the other hand, a significant increase in the number of network bursts, that is, a coordinated electrical spiking within groups of neurons, is indicative of collective network behavior. An increase in network bursts amidst decreases in individual spikes, mean firing rate, and synchrony suggests that while overall activity and global baseline coordination are reduced, these effects may be compensated by increasing the instances of global synchronization across neurons forming a new network (15). The presence of desynchronized non-burst firing and partially synchronized bursts in developing networks of cortical neurons supports the notion of network compensation and adaptation (16), suggesting a Hebbian field. Synchronization of bursting neurons is a critical factor in understanding network behavior, and it has been shown that burst firing can promote synchronization between interconnected loci in central nervous system networks (17). In summary, the observed changes in multi-electrode array (MEA) recordings following the treatment of primary cortical mouse neurons with COG-201 suggest a compensatory mechanism. Specifically, an increase in network bursts, despite decreases in individual spikes, mean firing rate, and synchrony, may indicate enhanced global synchronization within newly forming neuronal networks. This contrasts with the spontaneous global synchronization observed in all neurons treated with scrambled-AAV9-shRNA, which suggests the absence of distinct neuronal networks. This adaptive response at the network level may have implications for conditions such as anxiety and memory impairments.

An important caveat of the current study is connecting the MEA data with the underlying behavioral observations of a decrease in anxiety and improvement in memory. In the current study, we focused on cortical neurons; however, important neural networks implicated in memory and anxiety are found in the hippocampus and other subcortical areas including the interpeduncular nucleus (IPN). Previously, we identified a general pattern of guide RNA expression in the CA2/CA3 regions of the hippocampus in mice treated with CRISPR/Cas9 (10). Additionally, there was

a noticeable reduction in 5-HT<sub>2A</sub> receptor expression, particularly in the apical dendrites of glutamatergic neurons. Previous research has documented the presence of 5-HT<sub>2A</sub> receptor mRNA in the CA3 region of the hippocampus (18, 19). As the 5HT-2A receptor is excitatory, its downregulation in the apical dendrites may enhance memory by influencing hippocampal neuronal oscillatory rhythms (20, 21). In the context of the current study, projections to the apical dendrites of CA3 pyramidal neurons could originate from the cortex, particularly the entorhinal cortex, which is essential for sensory integration and memory formation. In terms of how our molecular findings could connect behaviorally to enhanced memory, it is essential to consider the broader neural circuits involved. The hippocampus plays a critical role in memory formation and anxiety regulation. Previous studies, including our own, have shown that the CA2/CA3 regions of the hippocampus are vital for these processes. Our findings have demonstrated a reduction in 5-HT<sub>2A</sub> receptor expression in the apical dendrites of glutamatergic neurons. The 5-HT<sub>2A</sub> receptor is known to be excitatory, and its downregulation can modulate hippocampal neuronal oscillatory rhythms, which are crucial for memory consolidation. The CA3 region, in particular, receives projections from the entorhinal cortex, which is essential for sensory integration and memory formation. The findings of reduced 5-HT<sub>2A</sub> receptor expression suggest a potential mechanism where altered serotonergic signaling in the hippocampus can influence cortical inputs, thereby enhancing memory functions. This aligns with the observed behavioral improvements in the current study.

We have also previously demonstrated a decrease in 5-HT<sub>2A</sub> receptor density in the IPN (10), an area implicated as a major connectome for stress-mediated pathways (22). Serotonergic cortical neurons are known to connect to the IPN via the habenula pathway (23, 24). Therefore, the downregulation of the 5-HT<sub>2A</sub> receptor in IPN neurons, along with a corresponding decrease in electrical excitability, could lead to a reduction in anxiety-related behaviors. Together with the effects of these cortical projections, however, we cannot exclude a possible modulatory role of 5-HT<sub>2A</sub> receptors expressed on local intrahippocampal interneurons that regulate the firing of pyramidal hippocampal subfield neurons, a role not specifically addressed in the current study. Previous studies have demonstrated that 5-HT<sub>2A</sub> receptors on GABAergic interneurons stimulate GABA release, and thereby have an important role in regulating network activity and neural oscillations in the amygdala and hippocampal region (25–27).

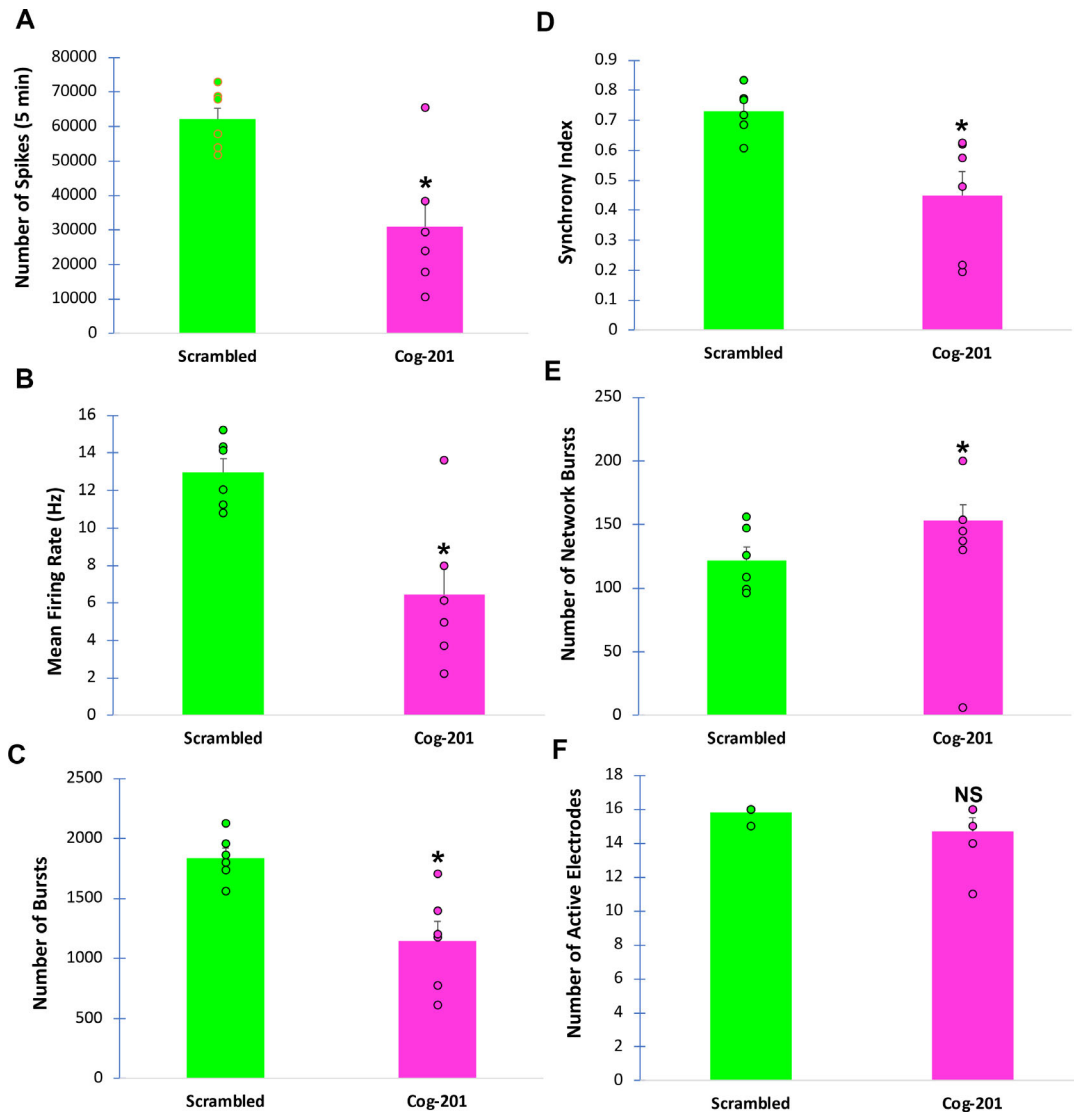


**Figure 5.** *In vitro* exposure of primary mouse cortical neurons with AAV9-mHTR2A-shRNA leads to a decrease in spontaneous electrical activity. MEA analysis was performed in mouse cortical neurons following treatment with either COG-201 (red bars, labeled “shRNA”) or a scrambled shRNA version (black bars, labeled “Scram”) at a MOI of  $2 \times 10^5$ . Neurons were treated at day 6 and MEA analyses were performed on day 16. (A–F) Quantification of MEA analysis showing the number of spikes over 5 minutes (A), mean firing rate (B), the number of bursts (C), the synchrony index (D), which indicates a unitless measure of synchrony between 0 and 1. Values closer to 1 indicate higher synchrony, the number of network bursts defined as a cluster of spikes across all electrodes (E), the synchrony index, which indicates a unitless measure of synchrony between 0 and 1 (values closer to 1 indicate higher synchrony), and the number of active electrodes (F). Exposure of neurons to  $2 \times 10^5$  MOI led to a significant decrease in the number of spikes (50% decrease compared to scrambled controls,  $p$ -value = .002) (A), the mean firing rate (50% decrease,  $p$ -value = .002) (B), in the number of bursts (27% decrease,  $p$ -value = .015), (C), and a decrease in the synchrony index (38% decrease compared to vehicle controls,  $p$ -value = .005) (D). An increase in the number of network bursts was observed (20% increase,  $p$ -value = .04) (E). For the number of active electrodes, there was no significant difference between the two groups (F),  $p$ -value = .09. Data represent  $N$  of 6 for all parameters,  $\pm$ S.E.M.

## Conclusions

Our study provides compelling evidence that COG-201 *in vivo* improves memory compared to vehicle control through a potential combined action of improving retention and lowering anxiety. *In vitro*, COG-201 led to a significant knockdown of the 5-HT<sub>2A</sub> receptor at both mRNA and protein levels in primary mouse cortical neurons, as confirmed by real-time qPCR, Western blot analysis, and immunocytochemistry. The reduction in receptor expression correlated with a decrease in neuronal excitability, as indicated by MEA assessments of electrical activity. Specifically, a significant reduction in spikes, mean firing rate, and synchrony index, coupled with an increase in network bursts, implies that COG-201 induces a reduction in overall excitability. However, the increased num-

ber of network bursts also suggests a compensatory mechanism within the neural network, that potentially enhances global synchronization. Our interpretation is that the increased network bursts in neurons with reduced 5-HT<sub>2A</sub> expression at baseline, is indicative of a newly formed neuronal network that has the potential of also increasing long-term potentiation. While this hypothesis can only be confirmed by further experiments, for example, applying electrical stimuli to *in vitro* neurons, thus mimicking the *in vivo* effects of the integration of sensory information. Nonetheless, these findings are aligned with previous behavioral observations of reduced anxiety and improved memory following COG-201 administration and underline the potential of COG-201 as an effective therapeutic agent (10). By elucidating some of the functional consequences



of 5-HT<sub>2A</sub> receptor knockdown, this study provides a critical link between molecular changes and the resultant alterations in neural circuitry that underpin the observed behavioral outcomes. Future research is warranted to explore the precise mechanisms by which COG-201 modulates network behavior and to assess the impact of these findings on therapeutic strategies for disorders including MCI that is characterized by anxiety and memory impairments. However, the current study utilizing mice to assess the efficacy of COG-201 is not without its' limitations. While these animal models are informative, there are significant physiological and genetic differences between rodents and humans that may affect the translatability of these findings to human therapeutics. In this context, the intranasal delivery of shRNA (COG-201) in animal models may not directly translate to humans due to differences in nasal anatomy and absorption efficiency. More research is needed to determine whether this delivery method is viable for human patients. Therefore, conducting studies in larger animal models that are more physiologically similar to humans (e.g., non-human primates) could provide better insights into the potential translational impact of COG-201.

In conclusion, if COG-201 proves effective in humans, it could offer a new treatment option for patients with conditions like MCI, which often involve anxiety and memory problems. This would be particularly beneficial given the limited treatment options currently available.

#### Declaration of Interests

J.L.M., B.J.L. and D.R. are co-founders of Cognigenics, members of its scientific advisory board, and hold equity in the company. T.T.R. is a part-time consultant serving as Director of Preclinical Research at Cognigenics and in addition to receiving a salary, owns shares of the company's common stock and options for common shares. F.M. is a part-time consultant serving as Chief Science Officer at Cognigenics, Inc., and is a member of its scientific advisory board.

#### Author Contributions

T.T.R., D.R., and F.M. designed research, analyzed and interpreted data and wrote the manuscript. All other authors reviewed the results and approved the final version of the manuscript. All experiments were carried out independently by contract research organizations.

#### Funding Statement

This research received no specific grant from any funding agency in the public, commercial, or not-for-profit sectors.

#### Generative Artificial Intelligence Statement

Generative artificial intelligence was not used to write the manuscript, but instead was used as a final tool to improve a human-generated text.

#### Acknowledgments

We thank our research partners at Neurofit and Creative Biolabs for their insightful suggestions and experimental expertise.

#### References

- Sachdev PS, Lipnicki DM, Kochan NA, Crawford JD, Thalamuthu A, Andrews G, et al. The prevalence of mild cognitive impairment in diverse geographical and ethnocultural regions: the COSMIC collaboration. *PLoS One*. 2015;10(11):e0142388. DOI: [10.1371/journal.pone.0142388](https://doi.org/10.1371/journal.pone.0142388). PMID: 26539987; PMCID: [PMC4634954](https://pubmed.ncbi.nlm.nih.gov/PMC4634954/)
- Chen C, Hu Z, Jiang Z, Zhou F. Prevalence of anxiety in patients with mild cognitive impairment: a systematic review and meta-analysis. *J Affect Disord*. 2018;236:211–21. DOI: [10.1016/j.jad.2018.04.110](https://doi.org/10.1016/j.jad.2018.04.110). PMID: 29747139
- Fire A, Xu S, Montgomery MK, Kostas SA, Driver SE, Mello CC. Potent and specific genetic interference by double-stranded RNA in *Caenorhabditis elegans*. *Nature*. 1998;391(6669):806–11. DOI: [10.1038/35888](https://doi.org/10.1038/35888). PMID: 9486653
- Holm A, Hansen SN, Klitgaard H, Kauppinen S. Clinical advances of RNA therapeutics for treatment of neurological and neuromuscular diseases. *RNA Biol*. 2022;19(1):594–608. DOI: [10.1080/15476286.2022.2066334](https://doi.org/10.1080/15476286.2022.2066334). PMID: 35482908; PMCID: [PMC9067473](https://pubmed.ncbi.nlm.nih.gov/PMC9067473/)
- Weisstaub NV, Zhou M, Lira A, Lambe E, Gonzalez-Maeso J, Hornung JP, et al. Cortical 5-HT<sub>2A</sub> receptor signaling modulates anxiety-like behaviors in mice. *Science*. 2006;313(5786):536–40. DOI: [10.1126/science.1123432](https://doi.org/10.1126/science.1123432). PMID: 16873667
- Celada P, Puig MV, Martín-Ruiz R, Casanovas JM, Artigas F. Control of the serotonergic system by the medial prefrontal cortex: potential role in the etiology of PTSD and depressive disorders. *Neurotox Res*. 2002;4(5-6):409–19. DOI: [10.1080/10298420290030550](https://doi.org/10.1080/10298420290030550). PMID: 12754155
- Cohen H. Anxiolytic effect and memory improvement in rats by antisense oligodeoxynucleotide to 5-hydroxytryptamine-2A precursor protein. *Depress Anxiety*. 2005;22(2):84–93. DOI: [10.1002/da.20087](https://doi.org/10.1002/da.20087). PMID: 16149040
- Jaggar M, Weisstaub N, Gingrich JA, Vaidya VA. 5-HT<sub>2A</sub> receptor deficiency alters the metabolic and transcriptional, but not the behavioral, consequences of chronic unpredictable stress. *Neurobiol Stress*. 2017;7:89–102. DOI: [10.1016/j.ynstr.2017.06.001](https://doi.org/10.1016/j.ynstr.2017.06.001). PMID: 28626787; PMCID: [PMC5470573](https://pubmed.ncbi.nlm.nih.gov/PMC5470573/)
- Naghdi N, Harooni HE. The effect of intrahippocampal injections of ritanserin (5HT<sub>2A/2C</sub> antagonist) and granisetron (5HT<sub>3</sub> antagonist) on learning as assessed in the spatial version of the water maze. *Behav Brain Res*. 2005;157(2):205–10. DOI: [10.1016/j.bbr.2004.06.024](https://doi.org/10.1016/j.bbr.2004.06.024). PMID: 15639171
- Rohn TT, Radin D, Brandmeyer T, Seidler PG, Linder BJ, Lytle T, et al. Intranasal delivery of shRNA to knockdown the 5HT<sub>2A</sub> receptor enhances memory and alleviates anxiety. *Translational psychiatry*. 2024;14(1):154. DOI: [10.1038/s41398-024-02879-y](https://doi.org/10.1038/s41398-024-02879-y). PMID: 38509093; PMCID: [PMC10954635](https://pubmed.ncbi.nlm.nih.gov/PMC10954635/)
- Rohn TT, Radin D, Brandmeyer T, Linder BJ, Andriambelison E, Wagner S, et al. Genetic modulation of the HTR<sub>2A</sub> gene reduces anxiety-related behavior in mice. *PNAS Nexus*. 2023;2(6):pgad170. DOI: [10.1093/pnasnexus/pgad170](https://doi.org/10.1093/pnasnexus/pgad170). PMID: 37346271; PMCID: [PMC10281383](https://pubmed.ncbi.nlm.nih.gov/PMC10281383/)
- Kim JE, Chae S, Kim S, Jung YJ, Kang MG, Heo W, et al. Cerebellar 5HT<sub>2A</sub> receptor mediates stress-induced onset of dystonia. *Sci Adv*. 2021;7(10):eabb5735. DOI: [10.1126/sciadv.abb5735](https://doi.org/10.1126/sciadv.abb5735). PMID: 33658190; PMCID: [PMC7929497](https://pubmed.ncbi.nlm.nih.gov/PMC7929497/)
- Komlósi G, Molnár G, Rózsa M, Oláh S, Barzó P, Tamás G. Fluoxetine (prozac) and serotonin act on excitatory synaptic transmission to suppress single layer 2/3 pyramidal neuron-triggered cell assemblies in the human prefrontal cortex. *J Neurosci*. 2012;32(46):16369–78. DOI: [10.1523/JNEUROSCI.2618-12.2012](https://doi.org/10.1523/JNEUROSCI.2618-12.2012). PMID: 23152619; PMCID: [PMC3752144](https://pubmed.ncbi.nlm.nih.gov/PMC3752144/)
- Brill J, Shao Z, Puche AC, Wachowiak M, Shipley MT. Serotonin increases synaptic activity in olfactory bulb glomeruli. *J Neurophysiol*. 2016;115(3):1208–19. DOI: [10.1152/jn.00847.2015](https://doi.org/10.1152/jn.00847.2015). PMID: 26655822; PMCID: [PMC4808087](https://pubmed.ncbi.nlm.nih.gov/PMC4808087/)
- Tajima S, Mita T, Bakkum DJ, Takahashi H, Toyozumi T. Locally embedded presages of global network bursts. *Proc Natl Acad Sci U S A*. 2017;114(36):9517–22. DOI: [10.1073/pnas.1705981114](https://doi.org/10.1073/pnas.1705981114). PMID: 28827362; PMCID: [PMC5594667](https://pubmed.ncbi.nlm.nih.gov/PMC5594667/)
- Maeda E, Robinson HP, Kawana A. The mechanisms of generation and propagation of synchronized bursting in developing networks of cortical neurons. *J Neurosci*. 1995;15(10):6834–45. DOI: [10.1523/JNEUROSCI.15-10-06834.1995](https://doi.org/10.1523/JNEUROSCI.15-10-06834.1995). PMID: 7472441; PMCID: [PMC6578010](https://pubmed.ncbi.nlm.nih.gov/PMC6578010/)
- Jiang H, Fang D, Kong LY, Jin ZR, Cai J, Kang XJ, et al. Sensitization of neurons in the central nucleus of the amygdala via the decreased GABAergic inhibition contributes to the development of neuropathic pain-related anxiety-like behaviors in rats. *Mol Brain*. 2014;7:72. DOI: [10.1186/s13041-014-0072-z](https://doi.org/10.1186/s13041-014-0072-z). PMID: 25277376; PMCID: [PMC4201706](https://pubmed.ncbi.nlm.nih.gov/PMC4201706/)
- Lüttgen M, Ove Ogren S, Meister B. Chemical identity of 5-HT<sub>2A</sub> receptor immunoreactive neurons of the rat septal complex and dorsal hippocampus. *Brain Res*. 2004;1010(1-2):156–65. DOI: [10.1016/j.brainres.2004.03.016](https://doi.org/10.1016/j.brainres.2004.03.016). PMID: 15126129
- Chen H, Zhang L, Rubinow DR, Chuang DM. Chronic buspirone treatment differentially regulates 5-HT<sub>1A</sub> and 5-HT<sub>2A</sub> receptor mRNA and binding sites in various regions of the rat hippocampus. *Brain Res Mol Brain Res*. 1995;32(2):348–53. DOI: [10.1016/0169-328x\(95\)00098-d](https://doi.org/10.1016/0169-328x(95)00098-d). PMID: 7500848
- Vertes RP. Hippocampal theta rhythm: a tag for short-term memory. *Hippocampus*. 2005;15(7):923–35. DOI: [10.1002/hipo.20118](https://doi.org/10.1002/hipo.20118). PMID: 16149083
- Berens SC, Horner AJ. Theta rhythm: temporal glue for episodic memory. *Curr Biol*. 2017;27(20):R1110–2. DOI: [10.1016/j.cub.2017.08.048](https://doi.org/10.1016/j.cub.2017.08.048). PMID: 29065291
- Sherafat Y, Bautista M, Fowler JP, Chen E, Ahmed A, Fowler CD. The interpeduncular-ventral hippocampus pathway mediates active stress coping and natural reward. *eNeuro*. 2020;7(6):ENEURO.0191-20.2020. DOI: [10.1523/ENEURO.0191-20.2020](https://doi.org/10.1523/ENEURO.0191-20.2020). PMID: 33139320; PMCID: [PMC7688303](https://pubmed.ncbi.nlm.nih.gov/PMC7688303/)
- Okamoto H, Agetsuma M, Aizawa H. Genetic dissection of the zebrafish habenula, a possible switching board for selection of behavioral strategy to cope with fear and anxiety. *Dev Neurobiol*. 2012;72(3):386–94. DOI: [10.1002/dneu.20913](https://doi.org/10.1002/dneu.20913). PMID: 21567982
- Stephenson-Jones M, Floros O, Robertson B, Grillner S. Evolutionary conservation of the habenular nuclei and their circuitry controlling the dopamine and 5-hydroxytryptophan (5-HT) systems. *Proc Natl Acad Sci U S A*. 2012;109(3):E164–73. DOI: [10.1073/pnas.1119348109](https://doi.org/10.1073/pnas.1119348109). PMID: 22203996; PMCID: [PMC3271889](https://pubmed.ncbi.nlm.nih.gov/PMC3271889/)
- Bombardi C, Di Giovanni G. Functional anatomy of 5-HT<sub>2A</sub> receptors in the amygdala and hippocampal complex: relevance to memory functions. *Exp Brain Res*. 2013;230(4):427–39. DOI: [10.1007/s00221-013-3512-6](https://doi.org/10.1007/s00221-013-3512-6). PMID: 23591691
- Wyskiel DR, Andrade R. Serotonin excites hippocampal CA1 GABAergic interneurons at the stratum radiatum-stratum lacunosum moleculare border. *Hippocampus*. 2016;26(9):1107–14. DOI: [10.1002/hipo.22611](https://doi.org/10.1002/hipo.22611). PMID: 27328460; PMCID: [PMC4996712](https://pubmed.ncbi.nlm.nih.gov/PMC4996712/)
- Zhang G, Stackman RW Jr. The role of serotonin 5-HT<sub>2A</sub> receptors in memory and cognition. *Front Pharmacol*. 2015;6:225. DOI: [10.3389/fphar.2015.00225](https://doi.org/10.3389/fphar.2015.00225). PMID: 26500553; PMCID: [PMC4594018](https://pubmed.ncbi.nlm.nih.gov/PMC4594018/)



**Publisher's note:** Genomic Press maintains a position of impartiality and neutrality regarding territorial assertions represented in published materials and affiliations of institutional nature. As such, we will use the affiliations provided by the authors, without editing them. Such use simply reflects what the authors submitted to us and it does not indicate that Genomic Press supports any type of territorial assertions.



**Open Access.** This article is licensed under the Creative Commons Attribution-NonCommercial-NoDerivatives 4.0 International License (CC BY-NC-ND 4.0). The license mandates: (1) Attribution: Credit must be given to the original work, with a link to the license and notification of any changes. The acknowledgment should not imply licensor endorsement.





(2) NonCommercial: The material cannot be used for commercial purposes. (3) NoDerivatives: Modified versions of the work cannot be distributed. (4) No additional legal or technological restrictions may be applied beyond those stipulated in the license. Public domain materials or those covered by statutory exceptions are exempt from these terms. This license does not cover all potential rights, such as publicity

or privacy rights, which may restrict material use. Third-party content in this article falls under the article's Creative Commons license unless otherwise stated. If use exceeds the license scope or statutory regulation, permission must be obtained from the copyright holder. For complete license details, visit <https://creativecommons.org/licenses/by-nc-nd/4.0/>. The license is provided without warranties.